Bose Centre for Advance Study and Research in Natural Sciences

University of Dhaka

Annual Report

Tuning Surface Properties of Porous Silica Nanoparticles for Application in Drug Loading

Duration: One Year

Project Director:

Dr. Saika Ahmed

Associate Professor

Department of Chemistry

University of Dhaka, Dhaka 1000

---

23 MAR

Director
Bose Centre for Advanced
Study & Research
Dhaka University

06.03.2023

Abstract

In recent years the interest for mesoporous nanomaterials have increased manifold due to the wonderful benefits these materials can provide in various applications, such as, as adsorbent, catalytic support, electrode material, separation media, in biomedical application, drug delivery etc. For obtaining best performance of mesoporous silica in various applications, it is a crucial need to optimize the synthesis parameters in order to achieve high surface area and high porosity. In this work, a well-known mesoporous silica, SBA-15, has been prepared by varying the concentration of the surfactant template, which is a non-ionic surfactant, pluronic P-123, with a view to finding the best condition for synthesizing silica in terms of the concentration of the surfactant template. The concentration of P-123 was varied from 50 to 400 times higher than the critical micellar concentration of P-123, i.e. 0.01 mM. The synthesized SBA-15 silica samples were characterized by BET surface analyzer to determine the mean pore size, specific surface area and total pore volume, Fourier transform infrared spectroscopy (FTIR) for molecular characterization, scanning electron microscope (SEM) for analyzing morphology and particle size distribution and X-ray diffraction (XRD) for phase identification. The surface area, total pore volume and mean pore diameter have been found to strongly depend on the concentration of the surfactants, which can be well explained by considering the alteration in the micelle structures of P-123 prior to silica synthesis.

Keywords: SBA-15, P-123, SEM, FT-IR, XRD

Introduction

Nanochemistry dealing with nanomaterials, nanoscience, nanotechnology, and nanostructures has been a fascinating domain of current research as well as indispensable to daily life. Nanochemistry is the understanding and control of matter having at least one dimension between approximately 1 and 100 nanometers, where some unique phenomena enable their novel applications. Encompassing nanoscale science, engineering and technology, nanotechnology involves imaging, measuring, modeling and manipulating matter at this length scale. One of the standard definitions of nanotechnology encompasses "research and technology development at the atomic, molecular, or macromolecular levels using a length scale of approximately 1-100 nm in any dimension; the creation and use of structures, devices, and systems that have novel properties and functions because of their small size, and the ability to control or manipulate matter on an atomic scale" **[1]**. This science uses methodologies from the synthetic chemistry and the materials chemistry to obtain nanomaterials with specific sizes, shapes, surface properties, defects, self-assembly properties, designed to accomplish specific functions and uses **[2]**. Nanomaterials can be created from virtually any material, such as metals, semiconductors and polymers, both in their amorphous and crystalline forms. The preparation, characterization and application of nanoparticles or nanostructured materials have received considerable attention, because of their properties. Since the nanoparticles usually exhibit unusual electronic, optical, magnetic, and chemical properties significantly different from those of the bulk materials due to their extremely small sizes and large specific surface areas, they have various potential applications (**Figure 1.1**) such as in catalysis, electronic, optical, and mechanical devices, magnetic recording media, superconductors, high-performance engineering materials, dyes, pigments, adhesives, photographic suspensions, drug delivery, and so on **[3]**. Nanoparticles (NPs) are now being used in the manufacture of scratchproof eyeglasses, crack-resistant paints, anti-graffiti coatings for walls, transparent sunscreens, stain-repellent fabrics, self-cleaning windows and ceramic coatings for solar cells.

Porous nanoparticles recently have been an attractive area of research due to the ability to control size of the guest nanoparticles by using different porous materials as supports. For example, porous silica and carbon are being used extensively for these type of industrial and research purposes. Porous materials generally employ the use of surfactants as templates to create pores of desired size range during their preparation.

Mesoporous silica is widely known for its ordered pores of meso-range size (2-10 nm) with high surface area, providing great opportunities in separation, catalysis, sensors, and synthesis of new nanostructured materials **[4]**. They also possess enhanced permeability and retention capability owing to their porous structure **[5]**.

The properties and application of mesoporous silica depends on their porosity parameters such as pore diameter, total pore volume as well as surface area. Surfactants are commonly used as structure-directing templates for creating pores during synthesizing mesoporous silica, which are removed after the synthesis by calcination at high temperatures to open the pores. Thus, pore size

and surface area are expected to be influenced significantly depending on the removal of surfactant after synthesis. Optimization of the synthesis conditions such as concentration of the surfactant template, calcinations temperature, and time etc. for obtaining the best surface properties, porosity and morphology of silica is a demanding question presently.

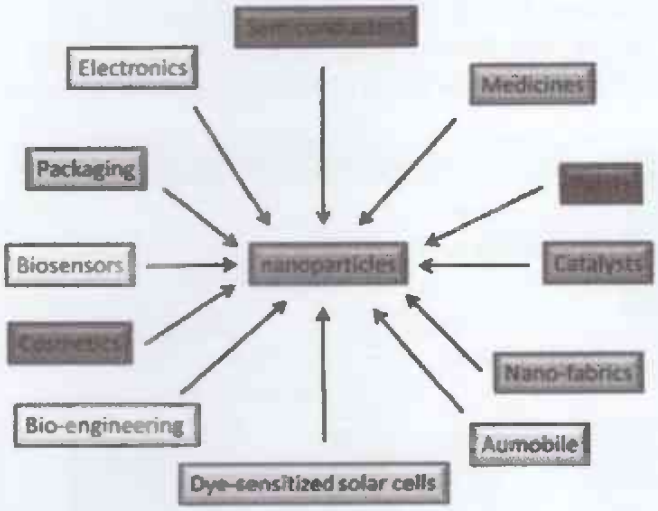


Figure 1.1: Diverse applications of nanoparticles.

Therefore, the objective of the present work is to study the effect of concentration of the surfactant P-123 on the surface properties and morphology of a mesoporous silica SBA-15 and thus, to optimize the concentration of P-123 surfactant template required for obtaining the best surface properties of silica. The objective also includes verifying the performance of the optimized SBA-15 silica samples as carriers for their application in drug loading.

Experimental

2.1 Materials

A non-ionic surfactant, pluronic P-123 (Aldrich) was used as received, as the template for synthesis of silica. Tetraethyl orthosilicate (TEOS), required for preparing silica, was received from Merck and used without further purification.

In order to avoid the influence of any impurities, extreme care was taken. To ensure proper cleaning the glass-wares were first washed with warm NaOH solution and then with excess nanopure water. Necessary care was taken to keep the solutions free from any dust particles.

2.2 Synthesis of silica

Mesoporous silica phases were synthesized by using nonionic surfactant as the structure-directing agents. In a typical preparation, the different types of non-ionic surfactants were dissolved in 1.6 M 150.0 g HCl solution with stirring at 35 °C; the concentrations of the

surfactants being such that after addition of TEOS, their concentrations reach the desired values, which are listed in **Table 2.1**. A representative calculation for the desired concentration of the surfactant, pluronic P-123, for synthesis of silica from P-123 having concentration 50 times higher than its CMC is shown in **Section 2.2.1.** 8.5g of TEOS was then added drop wise into that solution with stirring at 35 °C. The mixture was aged step wise at 35 and then 100 °C for two days without stirring. The mixture was then filtered; the residue was washed with water several times to remove Cl^- ions and dried at 110 °C for overnight. Finally, calcination was performed by slowly increasing the temperature from room temperature to 560 °C and then heating for 16 hours. The detailed procedure of synthesis of silica is shown in **Figure 2.1.**

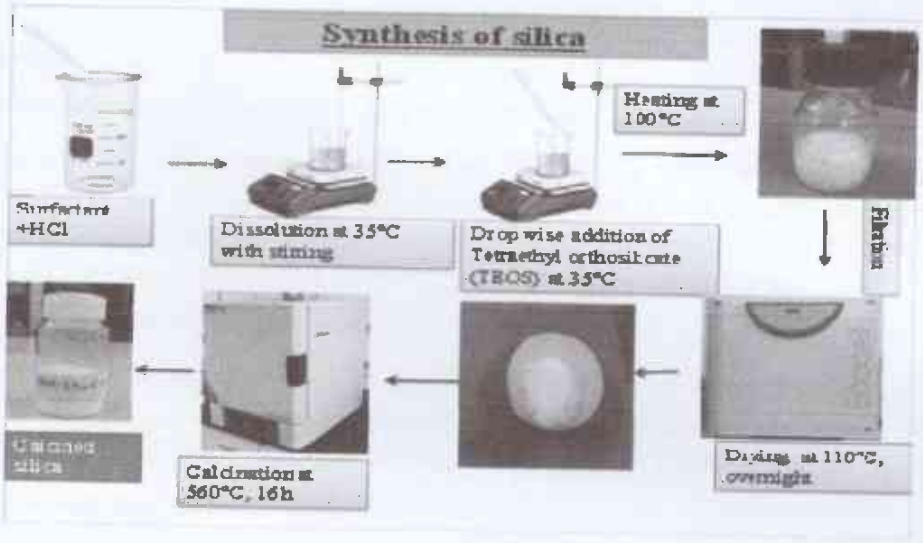


Figure 2.1: Synthesis procedure of SBA-15 using pluronic P-123 surfactant as template.

Table 2.1: The concentrations of surfactant template, P-123 used for synthesis of different silica.

CMC (mM)	Multiplication Factor, x	Final Concentration = x*CMC (mM)
0.01[13]	50	50×0.01= 0.5
	100	100×0.01= 1
	200	200×0.01= 2
	320	320×0.01= 3.2
	400	400×0.01= 4

2.2.1 Calculation of mass of pluronic P-123 required for obtaining desired concentration (50×CMC) of P-123 for synthesis of silica

Relative molar mass of pluronic P-123 = 5800 $gmol^{-1}$
CMC of P-123 = 0.01 mM = 0.01×10^{-3} M
Desired concentration of P-123 = $50 \times 0.01 \times 10^{-3}$ M = 0.0005 M
Total volume of solution containing 150 g HCl + 8.5 g TEOS = 147.5 mL + 9.1 mL
= 156.60 mL

Required mass of P-123 in 156.6×10^{-3} L solution = 0.0005 M × 156.6×10^{-3} L ×5800 $gmol^{-1}$
= 0.45414 g

2.4 Equipment

2.4.1 Fourier transform infrared (FT-IR) spectrometer

Perkin elmer FT-IR/NIR spectrometer (Frontier FT-IR/NIR, USA) was used for molecular characterization of the SBA-15 silica NPs. Prior to recording FT-IR spectra, the samples were mixed with KBr and made into pellets. The pellets thus made were put into the sample holder and the FT-IR spectra were recorded in the wave number range 4000-400 cm^{-1}.

2.4.2 Scanning electron microscope (SEM)

Morphology of the silica NPs could be determined by scanning electron microscope (Model JSM-6490LA). The scanning electron microscopic images of solid silica NPs were taken at an accelerating voltage of 20 KV with magnifications ranging from 10000-50000.

2.4.3 Particle size analyzer

Particle size of the silica NPs was measured by using Zetasizer Nano ZS90 (ZEN3690, Malvern instruments Ltd, UK). Dynamic light scattering (DLS) technique was employed to determine the particle size of silica NPs. A helium-neon laser of 632.8 nm wavelength was used and the measurements were made at a fixed scattering angle of 90°. Ethanol was used as a dispersant. Dispersions were sonicated prior to measurements. Hydrodynamic diameters were calculated from the measured diffusion coefficient by using the Stokes–Einstein model with the appropriate values of the solvent viscosity.

2.4.4 BET adsorption-desorption analyzer

Surface area and pore size distribution of the synthesized mesoporous silica calcined at different temperatures were measured by using BET surface area analyzer (Belsorp mini-II, BEL, Japan). N_2 gas adsorption-desorption isotherms were measured at different relative pressures, P/P_0, ranging from 0.01-0.99, on the surface of solid silica nanoparticles and used to determine surface area and pore size distribution of the mesoporous silica. N_2 gas adsorption was performed at -196° C, using liquid nitrogen as the cryogenic fluid and about 0.02 g of sample was taken in the sample cell for each measurement. Before measurement, the samples were pretreated at 120° C for at least 2 hours under N_2 gas flow by Belprep mini, BEL, Japan.

2.4.5 X-Ray diffractometer (XRD)

X-ray diffraction patterns of the prepared silica NPs were studied by using Philips PW-1830 X-ray diffractometer (XRD) and were recorded with XDC-700 Guinier Hagg focusing camera using Cu K□ radiation (wavelength= 1.540598 Å). Diffraction was carried out using Cu K□ radiation to analyze the phase composition with a wide range of Bragg angles, 2□ ranging from 10° to 80°. X-ray was exposed for 25 minutes on an image plate for each sample. Image plate was scanned using HD-CR 35 NDT/CR 35 NDT scanner to get intensity vs. line position in mm. Then it was converted to intensity vs. 2□ to get the complete diffraction pattern.

2.4.6 UV-visible spectrophotometer

Kinetic measurements and spectral analyses were carried out in a double beam Shimadzu UV – visible spectrophotometer, model UV- 1650 PC. Rectangular quartz cells of path length 1 cm were used throughout the investigation.

Results and Discussion:

3.1 Structural analysis of mesoporous silica

Non-ionic surfactant pluronic P-123 of five different concentrations (50-400 times their CMC value) in acidic solutions were used as templates for synthesizing porous silica, while TEOS was used as the silica source. After calcination at 560 °C for 16 hours, all the silica were characterized by measuring their FTIR spectra, XRD patterns, SEM images, particle size analysis by DLS studies and surface area/porosity analysis by measuring N_2 adsorption-desorption isotherms. Analysis of these studies and comparison between the silica samples prepared in the way described above are discussed in the following sections.

3.1.1 Fourier transform infrared (FTIR) spectra of silica

The Fourier transform infrared (FT-IR) spectra of silica synthesized using pluronic P-123 template were recorded in the wavenumber range of 4000-400 cm^{-1} in order to detect the different kinds of bonds present. IR grade KBr (100.0 mg) was thoroughly mixed with 1.0 mg of the sample and a pellet was made in order to record the spectra, which have been shown in **Figure 3.1** and assignments of the peaks are summarized in **Table 3.1.**

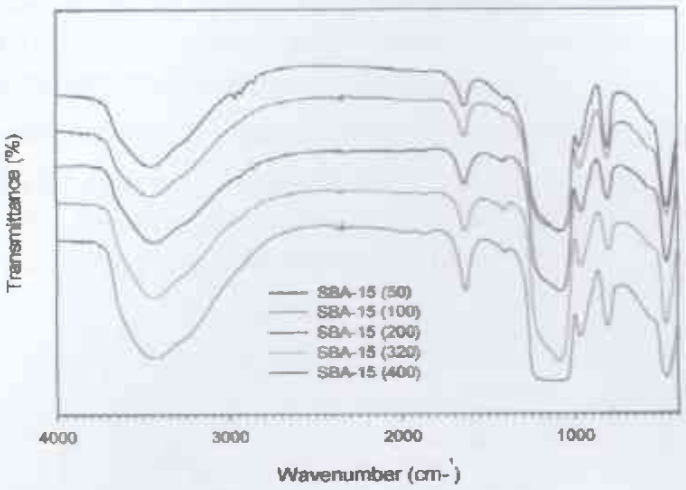


Figure 3.1: FTIR spectra of the silica synthesized from five different concentrations of pluronic P-123.

Table 3.1: Assignment of bands in the FTIR spectra of silica prepared using pluronic P-123 surfactant as template.

Wavenumber/cm^{-1}	Assignment of band
447	Si-O-Si (stretching)
801	Si-O-Si (bending)
947	Si-OH (stretching)
1093	Si-O-Si (stretching)
1630	O-H (bending)
3500	Si-OH (stretching)

According to **Figure 3.1,** FTIR spectra of all the porous silica nanoparticles synthesized using different concentrations of surfactant P-123 as templates show characteristic band of Si-O-Si at 447 cm^{-1} **[6-7]**. The absorption peak at around 3500 cm^{-1} corresponds to the stretching vibrations due to the presence of the surface silanol groups. The bending modes of vibrations forthe O-H group from silanol are observed at 1630cm^{-1}. The absorption band at 947 cm^{-1} is attributed to the stretching vibration of Si-OH **[8-11]**.

From the figure it is clear that all the silica samples synthesized from different concentrations of P-123 exhibit similar patterns of FTIR spectra. It is also noteworthy that the intensity of the peaks at 3500 and 1630 cm^{-1} coming from the silanol groups increase with increasing P-123 concentration, implying increasing amount of Si-OH groups.

3.1.2 X-ray diffraction patterns of silica synthesized from pluronic P-123

X-ray diffraction studies were used to identify the crystalline phases and to get an idea of the relative crystallite size of silica synthesized using pluronic P-123 of different concentrations as the templates. The diffraction patterns are presented in **Figure 3.2**.

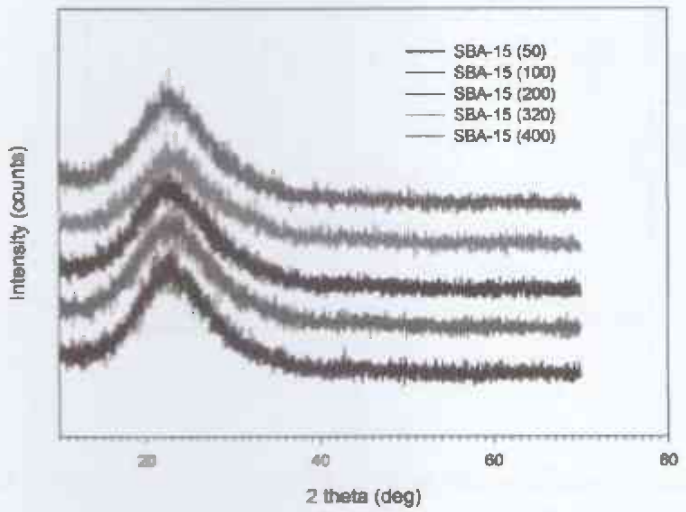


Figure 3.2: X-Ray diffraction patterns of silica nanoparticles synthesized using five different concentrations of P-123 surfactant template.

Figure 3.2 shows the XRD patterns of silica synthesized using pluronic P-123 surfactant template of different concentrations where all the samples exhibit a broad diffraction peak at a 2□ value of around 23° which can be indexed to the amorphous nature of the synthesized silica. In addition, the XRD peak at 23° seems to become slowly broader as the concentration of P-123 used to synthesize silica increases from 50 to 400 times the CMC value, indicating the silica particles to shift to more amorphous and homogeneous phase.

3.1.3 Particle size analysis of silica from pluronic P-123 by DLS technique

Dynamic light scattering (DLS) has several advantages for sizing nanoparticles and has been widely used to determine the hydrodynamic size of various nanoparticles owing to the short measurement time and non-invasive technique. In addition, since the scattering intensity is directly proportional to the sixth power of the particle radius, this technique is extremely sensitive towards the presence of small aggregates. Hence, erroneous measurement can be prevented quite effectively even with the occurrences of limited aggregation events.

Distribution of particle size (i.e. hydrodynamic diameter) of silica synthesized using different concentration of the P-123 surfactants were determined by DLS measurements. Distribution curve of the particle size of silica dispersed in ethanol is shown in **Figure 3.3**. All the SBA-15 silica samples show hydrodynamic diameter between a range from 200 to 600 nm. This large size of silica nanoparticles can be attributed to the measurement technique, since the DLS technique gives the hydrodynamic diameter of particles by considering them to be spherical in shape. Taking into consideration the ordered cylindrical shape of SBA-15, it is well-justified that DLS provided this large particle size.

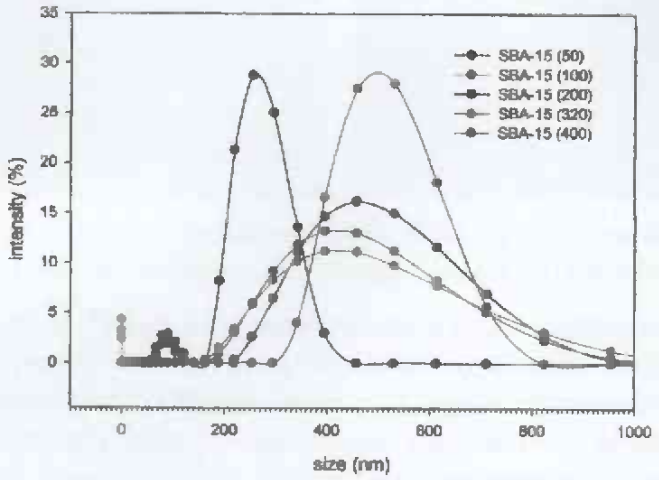


Figure 3.3: DLS distribution curve of particle diameter of SBA-15 silica nanoparticles synthesized using five different concentrations of P-123 surfactant.

3.1.4 Scanning electron microscopic images

The SEM images of different silica are shown in **Figure 3.4** which shows typical results of the studies of silica deposited on a carbon strip. The images show the morphology and particle size of the silica synthesized from different concentration of a surfactant.

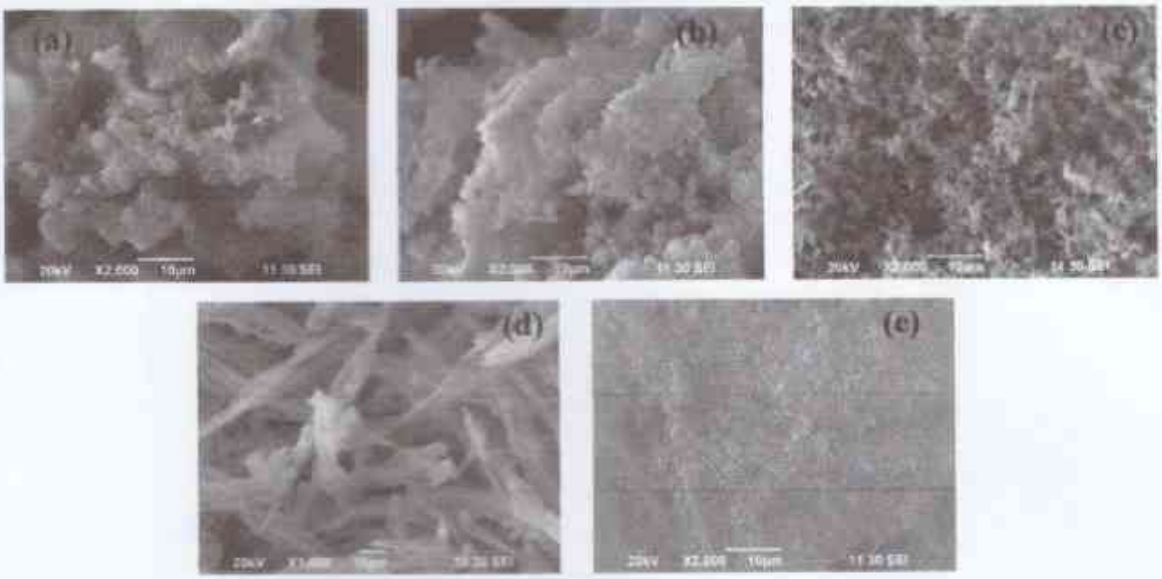


Figure 3.4: SEM images of silica synthesized using different concentrations of surfactant P-123 = (a) 50 times, (b) 100 times, (c) 200 times, (d) 320 times and (e) 400 times its CMC value.

The SEM images of silica (**Figure 3.4**) synthesized using P-123 at different concentrations show the morphology of porous silica nanoparticles. Silica synthesized from 50 and 100*CMC concentration of pluronic P-123 (**Figure 3.4 (a) and (b)**) do not show any regular shape and morphology. On the contrary, silica synthesized with pluronic P-123 of concentration 200, 320 and 400 times higher than CMC show well-defined, homogeneous structure. SEM image of silica synthesized from [P-123] = 320*CMC clearly shows porous structures. In addition, as the concentration is increased, the morphology shows a transition towards more amorphous phase, which is consistent with the results from XRD patterns (**Figure 3.2**). These results conclusively prove that the choice of the concentration of surfactant template plays a critical role in determing the morphology of silica.

3.1.5 Analysis of surface area and porosity from N_2 adsorption-desorption analysis

The silica synthesized from pluronic P-123 of different concentrations ranging from 50 to 400 times its CMC were characterized by BET isotherms obtained from N_2 gas adsorption-desorption measurements in order to analyze the surface area, pore volume and pore size distribution by using well known BET and BJH plots. Prior to the measurements, all the samples were pre-treated under N_2 gas flow at 120° C for at least 2 hours. The isotherms and BJH plots of these samples thus obtained are shown in **Figures 3.5** and **3.6** respectively.

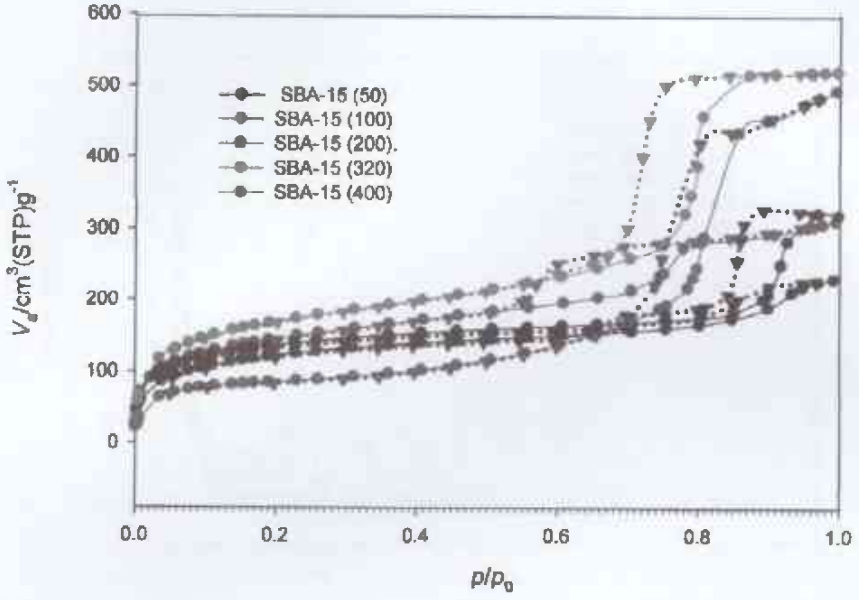


Figure 3.5: N_2 adsorption-desorption isotherms of different SBA-15 samples.

It can be clearly observed that the isotherms of SBA-15 silica that have been prepared by using five different concentrations of the surfactant pluronic P-123 represent Type-IV of the adsorption-desorption isotherms according to the IUPAC classification except the one synthesized using P-123 of 50 times its CMC. The presence of hysteresis in most of these isotherms is indicative of the porous nature of the substance. The shapes of the isotherms refer to the existence of mostly mesopores, along with some micropores.

From **Figure 3.5**, the SBA-15 sample synthesized using P-123 template with a concentration 50 times its CMC does not exhibit a significant amount of hysteresis; indicating low amount of pores in this sample. As the concentration of P-123 for templating silica increases, porosity starts to appear in the sample, as can be found in the silica sample containing [P-123] = 100*CMC. Silica from P-123 concentration 200, 320 and 400 times its CMC exhibit purely mesoporous nature as shown by the characteristic shape of hysteresis arising from mesopores. It is noteworthy here that the sample from [P-123] = 320*CMC shows the maximum amount of adsorption indicated by the adsorbed volume of N_2 and also by the largest hysteresis loop compared to the other silica samples. In addition, silica synthesized from [P-123] = 400*CMC show lower pore volume than the silica sample from [P-123] =320*CMC as evident by judging the relative amount of their hysteresis loops.

Figure 3.6 shows the typical Barrett, Joyner and Halenda (BJH) pore size distribution curves measured from the adsorption branch of the adsorption-desorption isotherms of SBA-15 silica nanoparticles synthesized from different P-123 concentrations.

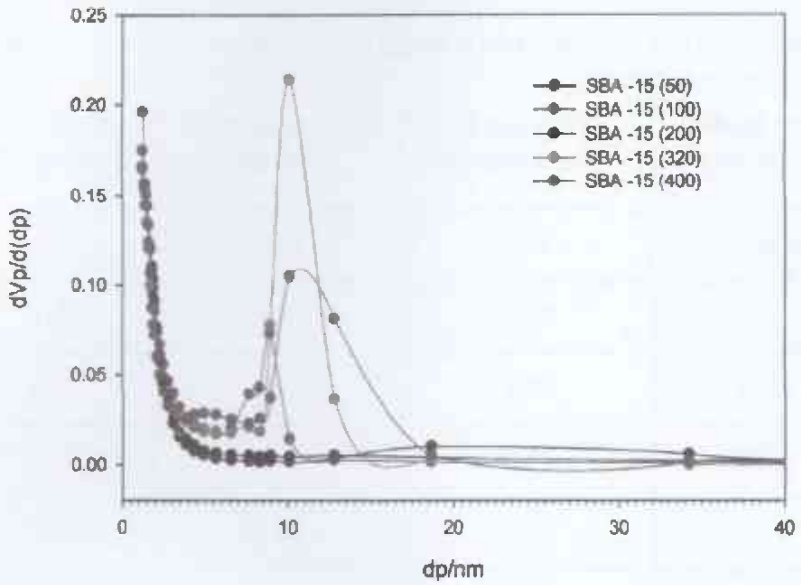


Figure 3.6: BJH pore size distribution curves of SBA-15 nanoparticles synthesized using five different concentrations of P-123 surfactant (based on adsorption branch).

From the BJH pore size distribution curves in **Figure 3.6**, it is clearly obvious that the silica sample from [P-123] = 50*CMC does not show a peak anywhere in the curve, thus lacking significant amount of porosity in the sample to be detected. On the other hand, all the other samples show well-defined peaks in their BJH curves between 9 and 20 nm indicating presence of mesopores in these samples. However, the silica that was synthesized using P-123 with a concentration 320 times its CMC shows the highest amount of adsorption which is consistent with the adsorption-desorption isotherms.

Analysis of the adsorption-desorption isotherms, corresponding BET and BJH plots of all the silica samples as described in the experimental section provided the specific surface area, total pore volume and mean pore diameter of the silica nanoparticles synthesized from different P-123 concentrations. The surface area, total pore volume and mean pore diameter thus calculated for different silica are tabulated in **Table 3.2**. These three parameters are also represented in graphical forms against the concentration of the surfactant P-123 in **Figures 3.7 (a), (b)** and **(c)**.

Table 3.2: BET specific surface area, total pore volume and mean pore diameter of SBA-15 silica nanoparticles synthesized from different concentrations of P-123 surfactant templates calculated from BET and BJH plots.

Here, concentration of P-123 = multiplication factor (x) * CMC of P-123 (= 0.01 mM)

Multiplication factor (x)	**Specific surface area /m^2g^{-1}**	**Total pore volume /cm^3g^{-1}**	**Mean pore diameter /nm**
50	454	0.36	1.3
100	526	0.48	9.1
200	503	0.49	18.0
320	613	0.80	10.6
400	320	0.76	10.1

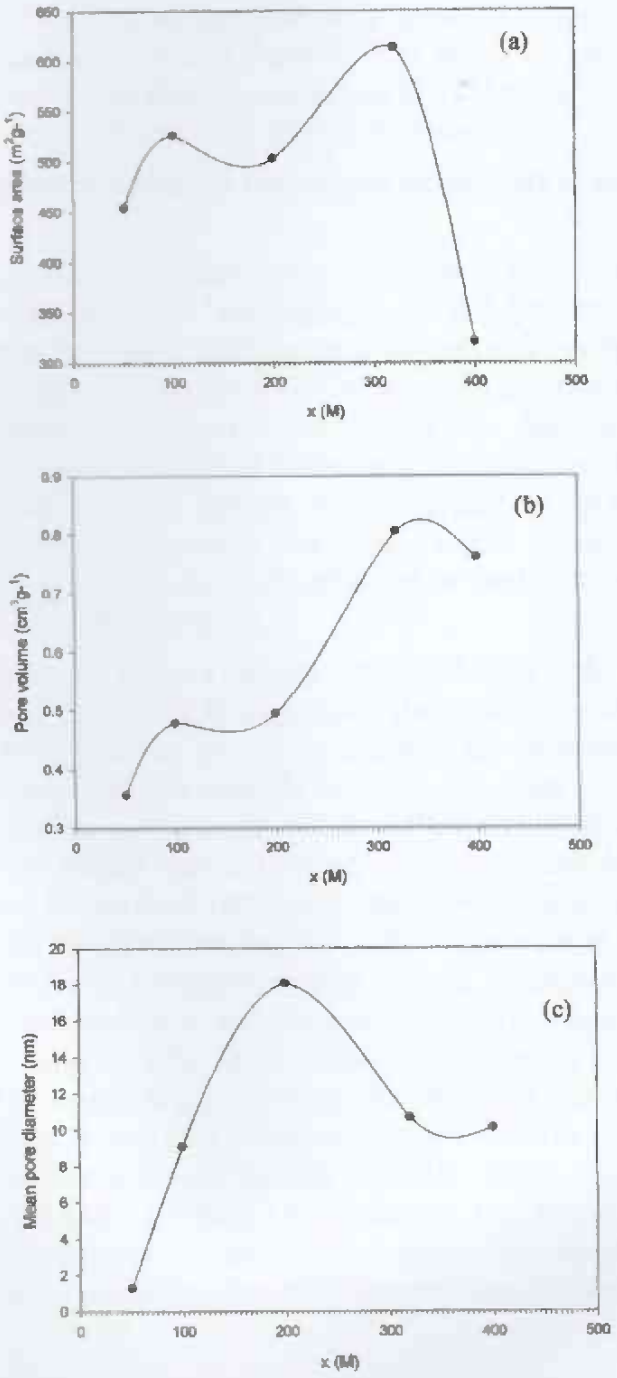


Figure 3.7: Effect of concentration of P-123 on the (a) surface area, (b) total pore volume and (c) mean pore diameter of the synthesized silica.

Table 3.2 and **Figure 3.7** show that the silica using [P-123] = 320*CMC exhibits the highest surface area (613 m^2g^{-1}) and pore volume (0.80 cm^3g^{-1}) while that using [P-123] = 400*CMC contains the lowest surface area (320 m^2g^{-1}) and 50*CMC shows the lowest pore volume (0.36 cm^3g^{-1}). In the case of mean pore diameter, silica from [P-123] = 200*CMC shows the highest value, whereas that from [P-123] = 50*CMC displays the lowest one.

3.2 Effect of concentration of surfactant template on the porosity as well as surface area of SBA-15 silica

At low concentrations, micelles are approximately spherical in shape. Other phases, including shapes such as ellipsoids, cylinders, and bilayers, are also possible at sufficiently high concentrations. The shape and size of a micelle are a function of the molecular geometry of its surfactant molecules and solution conditions such as surfactant concentration. In this work, the concentration of surfactant was changed to alter the porosity and surface area of different mesoporous silica which were synthesized using those surfactant micelles as pore-directing templates. Here non-ionic surfactant pluronic P-123 was used as the template. The critical micellar concentration of P-123 in aqueous HCl solution is 0.01 mM at 35°C temperature **[6]** Hence, the concentration of P-123 is extremely important for the formation of micelles and thus to obtain desired shape and porosity of silica.

The variations in the results for SBA-15 samples synthesized using P-123 surfactant at different concentrations above their CMC might be explained if the picture of micellization process of P-123 in solution prior to the synthesis of silica is looked at and taken into consideration. From analysis of the adsorption results, it might be expected that when [P-123] = 50*CMC, the micelles of P-123 are spherical,smaller in size and not sufficiently high in number, which may be speculated from the low surface area and lowest pore volume and pore diameter of their corresponding silica samples. As the P-123 concentration increases in the solution up to [P-123] = 320*CMC, number and size of micelles increase, which might result in aggregated cylindrical clusters of spherical micelles; eventually creating ordered cylindrical pores in silica in a homogeneous fashion, and leading to increasing surface area and pore volume in the silica sample. But as the concentration of P-123 is further increased above 320*CMC, some of the micelles coalesce and re-arrange to give micelles with ellipsoidal shapes, which consequently produces silica with lower surface area and pore volume. It is worth mentioning here that the pore diameter is not significantly changed than the 320*CMC sample, which is an indication that all the spherical micelles might not have been coalesced. This type of structural change in micelles, especially for non-ionic surfactants like P-123, is also reported and supported by literature **[12]**. This whole scenario described above is represented schematically in **Figure 3.8.**

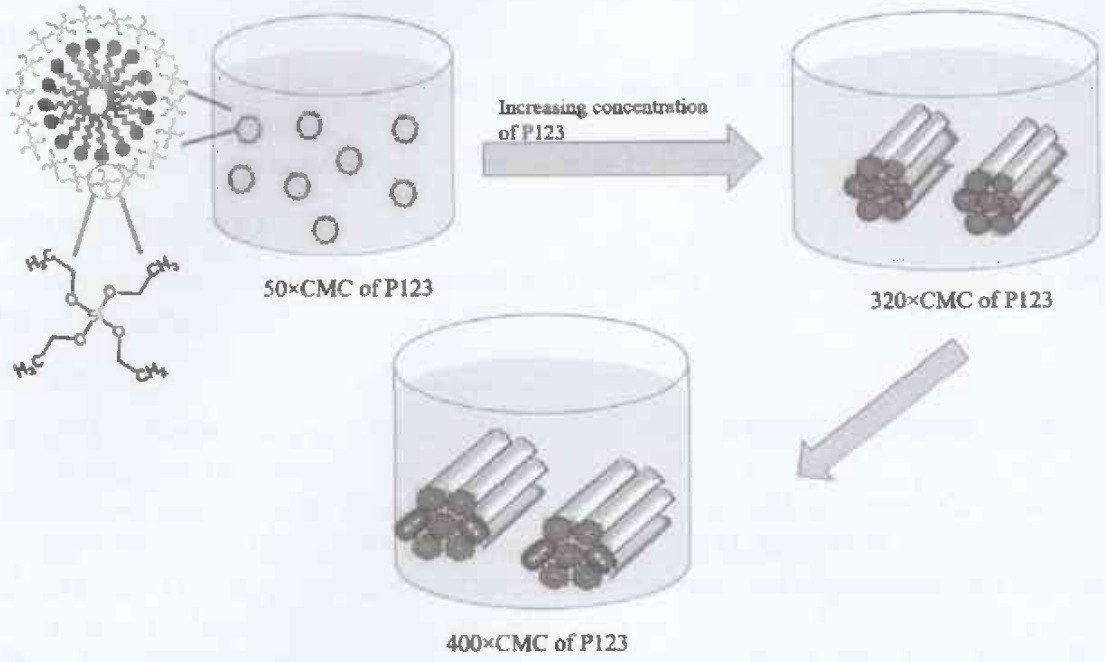


Figure 3.8: Schematic representation of the variation in micelle structures and shapes of pluronic P-123 at different concentrations above CMC during synthesis of SBA-15.

Conclusion

In this thesis, mesoporous silica nanoparticles (MSNs), namely SBA-15 have been synthesized by sol-gel method using P-123 surfactant as the structure-directing template for creating mesopores. The concentration of P-123 was varied between a range much higher than the CMC value of P-123 (from 50 to 400 times the CMC value) in order to analyze the effect of surfactant concentration on the surface area and porosity of SBA-15 silica and to find out the optimum surfactant concentration for obtaining the highest surface properties in silica. N_2 gas adsorption-desorption analyses show that the surface area and porosity of MSNs are found to be strongly influenced by the concentration of surfactant P-123. The amount of hysteresis, which is an indication of mesoporosity, was the highest found for the silica synthesized from a P-123 concentration 320 times its CMC value. The variation of surface area and porosity of the silica samples have been correlated with the structural change of the micelle shapes and structures they are templated from. The SEM images of SBA-15 nanoparticles synthesized from different concentration of surfactant P-123 show that the morphological shape of SBA-15 changes with the change of P-123 concentration, implying that the hexagonal shape of silica appeared slowly with the increasing concentration of surfactant. The XRD analysis of MSNs gives clear indication about the formation of silica and their amorphous phase.

Ongoing work

- Application of the SBA-15 samples with high and low surface properties in loading a familiar drug (aspirin)
- Comparison of the relative drug loading capacity of the different silica samples

Acknowledgement

The Bose Center for Advanced Study and Research in Natural Sciences is acknowledged by the author for its financial assistance.

References

1. EPA.; Nanotechnology White Paper; U.S. Environmental Protection Agency: Washington, DC, 2007.
2. *Nanochemistry: What Is Next?*, Ozin, Geoffrey A. and Cademartiri, Ludovico, 2009 Wiley-VCH Verlag, Weinheim small 2009, 5, No. 11, 1240–1244.
3. Dickson D P E, *Nanomaterials- Synthesis, Properties and Applications* Institute of Physics Publishing, Dirac House, UK, 459.
4. Fukuoka A.; Kimura J.; Oshio T.; Sakamoto T.; Ichikawa M.; *J. Am. Chem. Soc.*; **2007,** 129 (33), 10120.
5. Meng H.; Xue M.; Xia T.; Ji Z.; Tran D Y.; Zink J I.; Nel A E.; *J. Am. Chem. Soc.*; **2011,** 5(5), 4131.
6. Partyka S., Roquerol F., Roquerol J.; J. Colloid Interface Sci.; **1979**,68: 21.
7. Yongning H, Xiaoliang S., Lidun M .C.; *J. Appl. Chem.;* **1996,** 13, 92.
8. Babu K. S., Narayanan V.; *Chem Sci Trans.*; **2013,** 2: 33.
9. Geeetha D., Thilagavathi T.; *J. Nanomater. Biostruct.*; **2010**, 5: 297.
10. Prabhu Y. T., Rao, K. V., Kumar V. S. S; Kumari, B.S.; *Adv. Nanopart;*. **2013**, 2: 45.
11. Auffrkdic J. P.; Boultif A.; Langford J. I.; Louer D.; J. Am. Ceram. Soc.; **1995**, 78: 323.
12. Li Z., Gebner A., Richters J., Kalden J., Voss T., Kubel C., Taubert A.; *Adv. Mater.;* **2008**, 20: 1279.
13. http://openwetware.org/wiki/Critical_micelle_concentration(CMC).